A Versatile Microfluidic Tool for the 3D Culture of HepaRG Cells Seeded at Various Stages of Differentiation

Manon Boul
Université Paris Saclay, ENS Paris Saclay, CNRS SATIE, 4 avenue des Sciences, F91190 Gif-sur-Yvette
Nassima Benzoubir
UMR_S 1193 INSERM/Université Paris-Saclay, F94800 Villejuif
Antonietta Messina
UMR_S 1193 INSERM/Université Paris-Saclay, F94800 Villejuif
Rasta Ghasemi
Université Paris Saclay, Institut d'Alembert, ENS Paris Saclay, CNRS, F91190 Gif-sur-Yvette
Ismail Ben Mosbah
Biopredic International, Parc d'Affaires La Bretêche, 35760, Saint Grégoire
Jean-Charles Duclos-Vallée
APHP, Centre Hépato-Biliaire, Hôpital Paul Brousse, F94800 Villejuif
Anne Dubart-Kupperschmitt
UMR_S 1193 INSERM/Université Paris-Saclay, F94800 Villejuif
Bruno le Pioufle (bruno.le-pioufle@ens-paris-saclay.fr)
Université Paris Saclay, ENS Paris Saclay, CNRS LUMIN, F91190 Gif-sur-Yvette

Research Article

Keywords: 3D, cells, HepaRG, 2D

Posted Date: January 8th, 2021

DOI: https://doi.org/10.21203/rs.3.rs-138606/v1

Version of Record: A version of this preprint was published at Scientific Reports on July 7th, 2021. See the published version at https://doi.org/10.1038/s41598-021-92011-7.

A versatile microfluidic tool for the 3D culture of HepaRG cells seeded at various stages of differentiation

Manon Boul[1,2,3,4,5], Nassima Benzoubir[2,4], Antonietta Messina[2,4], Rasta Ghasemi[5], Ismail Ben Mosbah[6], Jean-Charles Duclos-Vallée[2,4,7], Anne Dubart-Kupperschmitt[2,4], and Bruno Le Piouffle[*3,4,5]

[1]Université Paris Saclay, ENS Paris Saclay, CNRS SATIE, 4 avenue des Sciences, F91190 Gif-sur-Yvette, France
[2]UMR_S 1193 INSERM/Université Paris-Saclay, F94800 Villejuif, France
[3]Université Paris Saclay, ENS Paris Saclay, CNRS LUMIN, F91190 Gif-sur-Yvette, France
[4]FHU Hépatinov, Centre Hépato-Biliaire, Hôpital Paul Brousse, F94800 Villejuif, France
[5]Université Paris Saclay, Institut d'Alembert, ENS Paris Saclay, CNRS, F91190 Gif-sur-Yvette, France
[6]Biopredic International, Parc d'Affaires La Bretêche, 35760, Saint-Grégoire
[7]APHP, Centre Hépato-Biliaire, Hôpital Paul Brousse, F94800 Villejuif, France
*Correspondence and requests for materials should be addressed to B.L-P. (email: bruno.le-piouffle@ens-paris-saclay.fr)

ABSTRACT

The development of livers-on-a-chip aims to provide pharmaceutical companies with reliable systems to perform drug screening and toxicological studies. To that end, microfluidic systems are engineered to mimic the functions and architecture of this organ. In this context we have designed a device that reproduces series of liver microarchitectures, each permitting the 3D culture of hepatocytes by confining them to a chamber that is separated from the medium conveying channel by very thin slits. We modified the structure to ensure its compatibility with the culture of hepatocytes from different sources. Our device was adapted to the migratory and adhesion properties of HepaRG cells at various stages of differentiation. To prevent hepatoblast-like cells from migrating out of the chambers, the slit height was decreased and the medium flow rate increased. Maintaining already differentiated and less adherent cells within the chambers required desensitisation of the system to pressure variations. Using this device, it was possible to keep the cells alive for more than 14 days, during which they achieved a 3D organisation and acquired or maintained their differentiation into hepatocytes. With its multiple micro-chambers for hepatocyte culture, this microfluidic device architecture offers a promising opportunity to provide new tools for drug screening applications.

Introduction

The use of animal models and two dimensional (2D) cell cultures usually fail to reproduce *in vivo* drug metabolism and liver toxicity in humans[1]. Indeed, the correspondence between animal and human models regarding hepatic drug toxicity only reaches 30 to 50%[1,2]. Furthermore, primary hepatocytes cultured under 2D conditions rapidly lose their functions and cannot offer a long term assessment of medicinal effects[3]. Lastly, hepatotoxicity is considered as one of the principal reasons for the withdrawal of FDA-approved drugs from the market[4]. The pharmaceutical industry therefore requires access to improved predictive models.

Culturing hepatocytes under flux and/or three dimensional (3D) conditions has been shown to improve their viability and functions[5]. For this reason, perfused hepatocyte culture systems

are currently seen as promising candidates to reflect liver functionality *in vitro*[6]. Because of their small size, liver-on-a-chip devices offer a convenient tool to culture hepatic cells under a flow and produce an adequate supply of high-throughput data for drug development[7,8]. Using such systems, cells are generally cultured as either 2D monolayers, spheroids or aggregates within an oversized chamber[9–14]. Several research groups have taken advantage of microfluidic techniques to reproduce the microarchitecture of the liver. In particular, a hepatocyte cord was mimicked on a chip[15,16]; the dimensions of the cell culture chamber and its proximity to a vascular channel were more similar to the *in vivo* situation than other systems. However, only a small number of rat primary hepatocytes were seeded and only their 2D organisation could be achieved using these devices.
The development of a model that can predict liver drug metabolism and be used for toxicity studies requires considerable accuracy and reproducibility. This is reliant on the quality of the hepatocytes used in the systems described above, but how to obtain an unlimited supply of high quality hepatocytes still needs to be clarified[6]. For this reason, it is necessary to develop a versatile device compatible with human hepatocytes from different sources (including primary cells, liver tumour-derived cell lines, and cells derived from induced pluripotent stem cells (iPSCs)) in order to compare their responses to drugs[1,6].

To better reflect the functions of the liver, we propose in this paper to combine the on-chip mimicking of hepatic-cord microarchitecture with the 3D culture of hepatocytes. We serially replicated this structure in order to observe and simultaneously culture tens of organised tissues using the same device. For the first time, this hepatocyte-cord-like microfluidic chip was used to culture the HepaRG cell line. Of all the human hepatic cell lines available, differentiated HepaRG cells are considered to be the most similar to human primary hepatocytes in terms of their functions and level of metabolic activity[6,17]. When seeded at low density, HepaRG cells are proliferative hepatoblast-like cells, but once they reach confluency, they undergo spontaneous differentiation into hepatocyte-like cells. This differentiation can be enhanced by adding dimethyl sulfoxide (DMSO) to the culture medium. Both hepatoblast- and hepatocyte-like HepaRG cells are already widely used for liver bioreactor applications[18,19] and to evaluate drug toxicity[20–23], respectively. The properties of hepatoblasts and hepatocytes from the HepaRG cell line were evidenced to differ in terms of their migration and adherence: this feature prompted us to adapt the structure and packaging of the chip accordingly, and the culture of these cells under flux for several weeks was then achieved. The viability and spontaneous differentiation of cells into hepatocytes were assessed in the microfluidic device, as was their 3D organisation.

Results

Design of the device

Our device was designed to reproduce the liver microarchitecture and was based on proposals previously described by Lee *et al.*[15] and Nakao *et al.*[16]: a cell culture chamber is surrounded by a medium conveying channel and both being linked by arrays of slits (**Fig. 1.a**). These elements mimic hepatic cords, liver sinusoids and the space of Disse, respectively. The slits enable oxygen and nutrients to diffuse to the cells while protecting them from high shear stress. Under our design, the height of the central chamber is optimised in order to promote the 3D organization of hepatocytes. To maximise the number of hepatic cords on a single microfluidic device, this unit structure is arranged as two parallel series of 20 hepatocyte culture chambers. Our device comprises two fluidic circuits that are interconnected via the slits: a medium flowing channel and a cell loading channel, to enable the seeding of multiple chambers (**Fig. 1.b**). These fluidic circuits are filled and controlled from the four outlets placed at the extremities of the microfluidic chip. Our initial device was designed with channel and slit heights of 25 and 5 µm (**Fig. 1.d**), respectively, so is thus referred to as the "25-5 µm device".

Behaviour of proliferative HepaRG cells in the chip

We first of all loaded HepaRG cells at a proliferative stage onto the device: we expected them to adhere to the glass and PDMS, proliferate and then completely fill the chambers. Because these cells have a diameter of around 17 µm[17], they were expected to organise themselves in 3D structures with stacks of two cells, and once they reached a high density to spontaneously differentiate into hepatocytes.

After loading the cells onto the 25-5 µm device and culturing them under static conditions, they were found to migrate out of the chambers through the slits (**Fig. 2.a**). This had not been observed in the case of rat primary hepatocytes[16]. Indeed, the latter did not proliferate and because of their differing rigidity and size, behaved unlike the human cell lines in our chip. The absence of HepaRG cells from the medium channel immediately after loading and the presence of nuclei within the slits after several hours of culture provided evidence of cell migration. Once inside the medium channel, the cells started to adhere, proliferate and fill the channel, which was not our objective. In addition, instead of organising themselves into 3D structures, the cells appeared to form a monolayer inside the chambers (**Fig. 2.b**). Ultimately, it was considered that this device was not suited to culturing the cells we were targeting, so its design was modified.

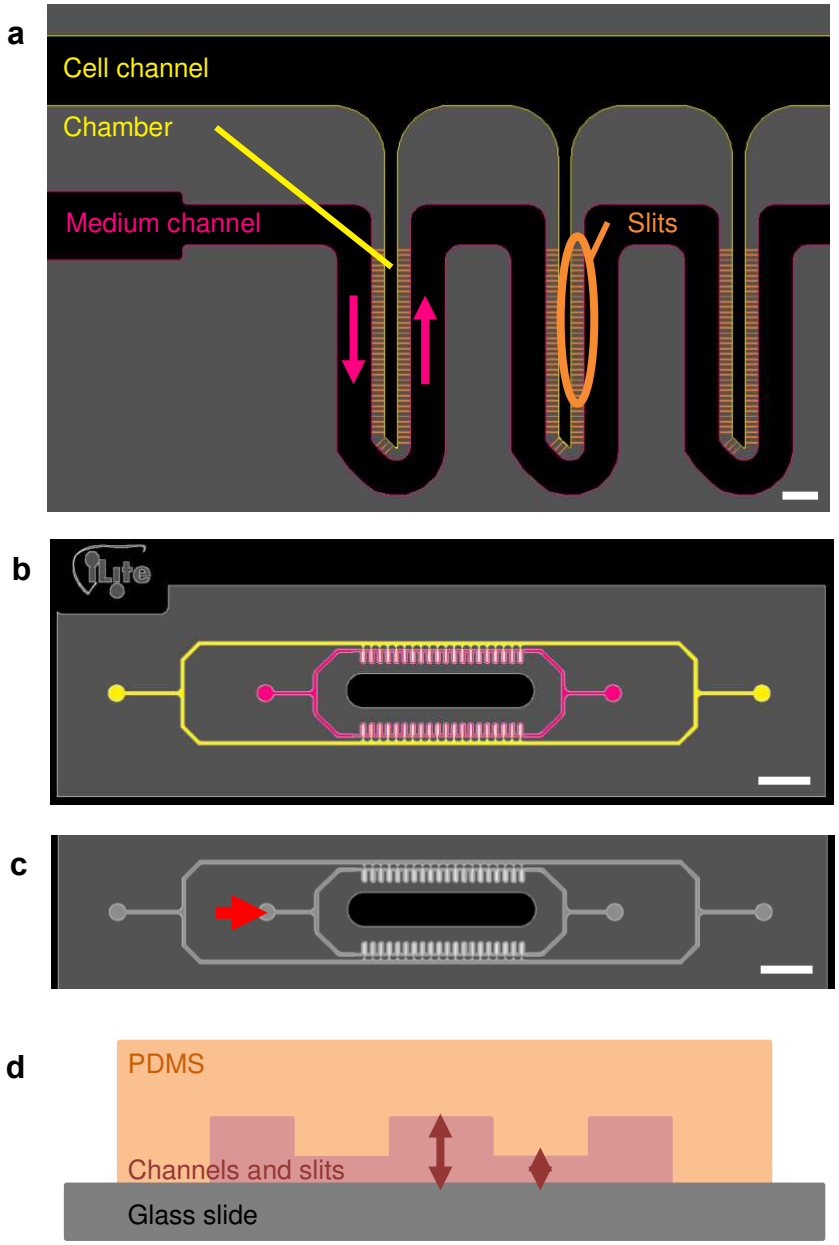

Figure 1. Design of the microfluidic device. **a**) Zoom on three chambers. The cell channel and hepatocyte chambers (yellow) communicate with the medium channel (pink) via an array of slits (orange). The direction of medium flow is represented by pink arrows. Scale bar = 100 µm. **b**) Top-down view of the design which comprises two fluidic circuits: in pink the medium channel and in yellow the cell channel. Scale bar = 3 mm. **c**) Fluidisation of the chip: the flow enters from one inlet of the medium channel (red arrow) and leaves via three outlets. Scale bar = 3 mm. **d**) Side-on diagram of the device: a polydimethylsiloxane (PDMS) chip (orange) is sealed to a glass slide (grey), thus creating microfluidic channels (pink). Depending on the different versions of the device, the slits are 2 or 5 µm high and the other channels are 25 or 40 µm high.

Device optimisation to prevent cell migration through the slits

Device modification

To prevent cell migration, the slit height was reduced to 2 µm and a different design was tested. Of the two series of 20 chambers in the device, one consisted of straight slits (as previously) while the other was made of discontinuous slits including 90° angles (**Fig. 2.c.ii**). Moreover, to favour the stacking of cells inside chambers, the channel height was increased to 40 µm. A new system, referred to as the "40-2 µm device", was thus produced.

Calculation of a theoretical flow rate range

The initial design of our device had been tested under static conditions which might have contributed to the migration of cells through the slits, but establishing a flow in the medium channel might help to prevent cell adherence and proliferation (**Fig. 1.c**). A flow rate range suitable for the culture of hepatocytes in the new device was determined by simulations. Analytical calculations showed that chambers with straight or discontinuous slits would have equivalent hydraulic resistivity (absolute difference of 2%), so simulations were performed on arrays of straight slits. During numerical simulations of the device, the presence of cells inside the chambers was not taken into account despite the fact that this might reduce fluid velocity. Our calculations therefore corresponded to the worst conditions considering the shear stress applied to cells. To determine the maximal flow rate value, the mapping of fluid velocity and shear stress inside the chambers was analysed. For an inflow of 400 nl/min, the mean fluid velocity inside the chambers was 5.53×10^{-5} m/s, one order of magnitude lower than in the medium channel (3.57×10^{-4} m/s). A fluid velocity gradient was evidenced within the chambers, while variations in velocity were also observed between successive chambers (**Fig. 3.a**). The flow velocity gradient inside the chambers was quantified along the y axis from their dead-end portion - connected to the medium channel through the slits – towards the outlet from the chamber - connected to the cell channel. Velocity was found to increase linearly with y in the dead-end portion of the chamber and reach a plateau at its outlet (**Supplementary Fig. S1**). Average fluid velocity also varied between the chambers, different from the first to the last reached by the medium (chambers 1 and 20 in **Fig. 3.a**, respectively), falling by around one order of magnitude (**Fig. 3.c**). The same trends and differences were also evidenced with respect to the shear stress values calculated on the surfaces of the chambers (**Supplementary Fig. S1**). These values were locally higher at slit/chamber interfaces but remained lower than 0.1 Pa on average, in the knowledge that 0.5 Pa is the maximum acceptable shear stress for hepatocytes[24] (**Fig. 3.b.c**). Thus, on the device, the higher shear stress value that needed to remain below 0.5 Pa was that found at the exit from the first chamber. In addition, the mean shear stress inside a chamber increased linearly with the flow rate. As a result of this, the maximum flow that could be imposed was 9.5 µl/min. To determine the minimal value of the flux that would keep the cells alive, we estimated the level of their oxygen supply, which was found to arise from its diffusion through polydimethylsiloxane (PDMS): independently of the flow rate applied, its concentration was above the hypoxic limit, considered to be 0.04 mol/m^3 (equivalent to 32 mmHg)[25–27], in all chambers (**Supplementary Fig. S2**). Even at a low flow rate, therefore, the cells would receive sufficient oxygen. Ultimately, it was decided that a flow rate lower than 9.5 µl/min was appropriate for the culture of hepatocytes on this device.

Migration of HepaRG hepatoblasts in the new chip

The 40-2 µm device was tested using flow rates ranging from 50 to 400 nl/min. Under these conditions, few nuclei were found outside the chambers or in the slits, and the few cells that reached the medium channel did not proliferate (**Fig. 2.b**). Although cell nuclei were no longer escaping through the slits, cytoplasmic extensions were nevertheless seen to elongate through the slits into the medium channel, as demonstrated by phalloidin staining (**Fig. 2.c.i**). Surprisingly, when compared to straight slits, discontinuous ones at 90° angles did not reduce these cytoplasmic extensions (**Fig. 2.c.ii**). Inside the 40 µm high channels, however, the cells did aggregate and stack. They could not be identified individually by phase contrast microscopy but appeared as quite round and darker structures corresponding to cell aggregates (**Fig. 2.b**). This channel height was thus better suited to enabling the cells to organise in 3D structures. This device was therefore used for the remainder of the study.

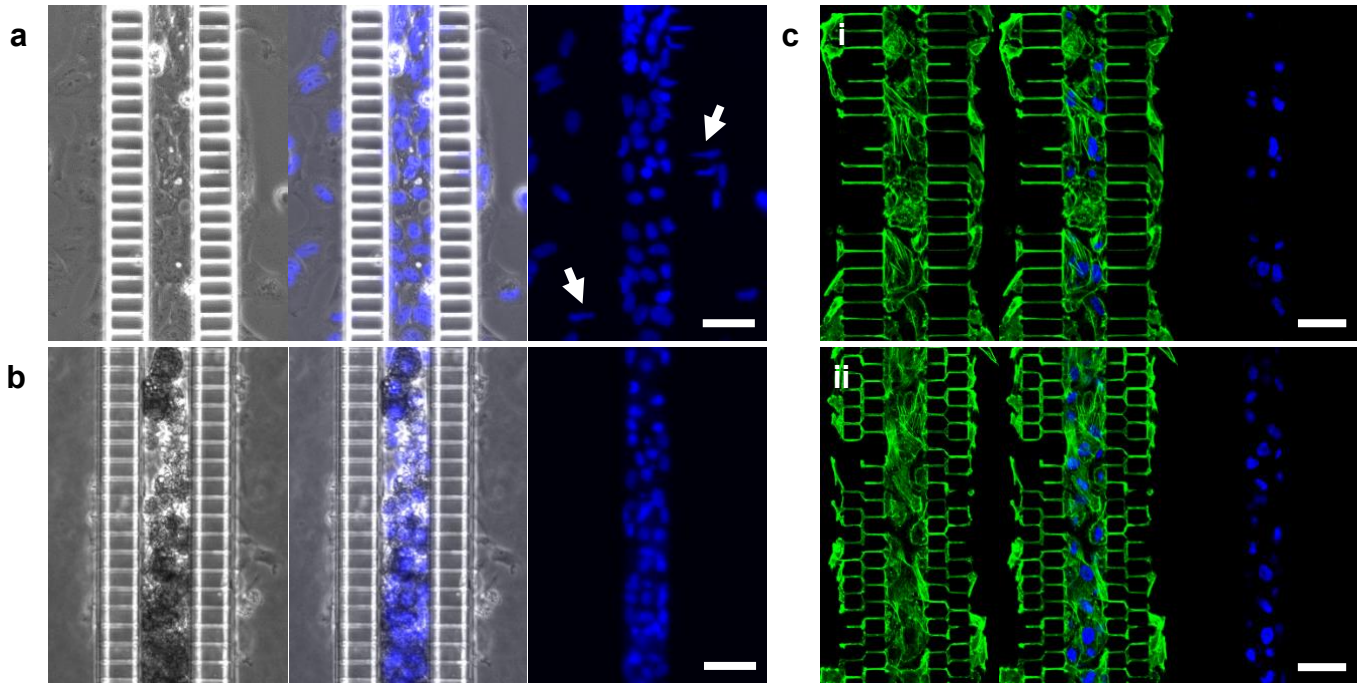

Figure 2. Evidence for the migration of proliferative HepaRG cells out of culture chambers determined by phase contrast imaging and fluorescent staining (blue: DAPI, green: phalloidin, staining cell nuclei and F-actin filaments, respectively). **a**) Epifluorescence microscope images of a chamber on the 25-5 µm device after 2 days under static conditions. The migration of cell nuclei through slits was observed (white arrows). **b**) Epifluorescence microscope images of a chamber on the 40-2 µm device after 14 days at 50 nl/min. **c**) Confocal microscope images of a chamber on the 40-2 µm device after 14 days at 50 nl/min: **i**) with straight slits or **ii**) with discontinuous slits. Scale bars = 40 µm.

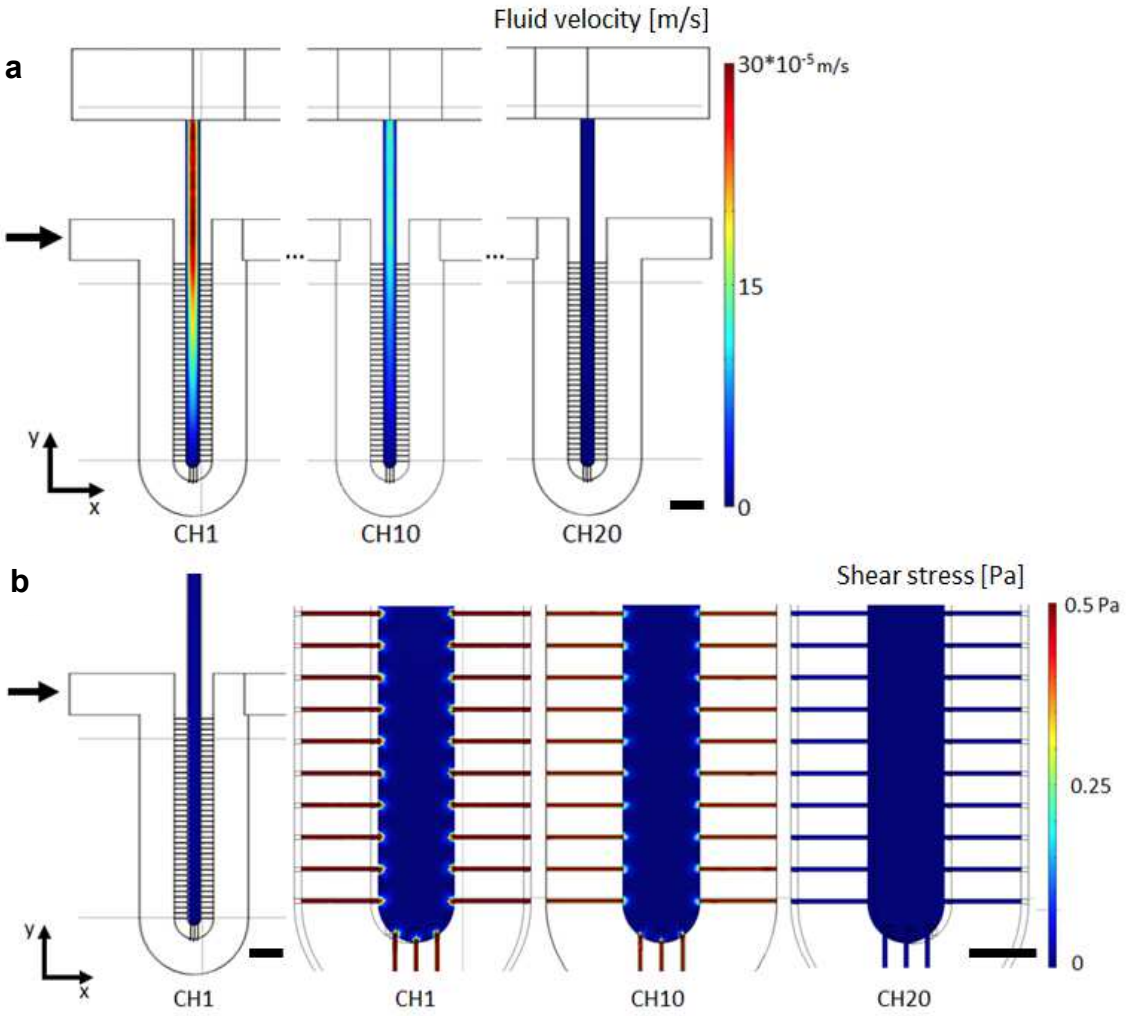

c

400 nl/min	Mean velocity [m/s]	Mean shear stress [Pa]
40-2 device		
Chamber n°1	9.08e-5	2.1e-2
Chamber n°10	3.98e-5	9.0e-3
Chamber n°20	1.97e-5	4.0e-4

Figure 3. Numerical modelling of the culture conditions for cells on the 40-2 µm chip. 3D COMSOL® simulation of 20 chambers in a series with straight slits, without any cells, at 37°C. The flow rate at the inlet (symbolized by black arrows) is 400 nl/min. At the three outlets the pressure is set at 0 Pa. **a**) Fluid velocity on the xy plan (z = 20 µm) for chambers 1, 10, and 20. Scale bar = 100 µm. **b**) Shear stress on the xy plan (z = 0 µm). Left-hand side: general view of the first chamber, scale bar = 100 µm. Right-hand side: zoom on the dead-end portion of chambers 1, 10, and 20. Scale bar = 40 µm. **c**) Table of the mean values for velocity and shear stress inside chambers 1, 10, and 20.

Further optimization to maintain HepaRG hepatocytes inside chambers

Behaviour of differentiated HepaRG cells loaded onto the chip

Compared to proliferative HepaRG cells, HepaRG hepatocytes adhered less to the substrate than to each other[28]. We therefore expected them to be more prone to forming aggregates in the chambers and less likely to invade the slits. However, once these cells were loaded into the 40-2 µm device, the pressure disturbances induced when connecting the tubes to establish the flow drove the cells out of the chambers (**Fig. 4.a**). Hydrostatic pressure variations induced by modifying the respective heights of the syringe and the device produced similar effects. Increasing the delay prior to fluidisation (from 6h to 24h), which might have improved cell adhesion to the substrate, was ineffective in preventing this phenomenon.

Desensitising the device to pressure disturbances

We calculated that a height difference of 20 cm between the syringe and the chip induced a flow of 4.6 µl/min within the medium channel. This flow was acceptable in terms of the shear stress induced when compared to the values obtained by the simulations but remained sufficient to expel poorly adherent cells from the chambers. To reduce the flux generated by these pressure disturbances, we added external flow resistance to our device, which consisted in a thin capillary tube. This was inserted between the syringe and the chip (**Supplementary Fig. S4**). We tested two capillary tubes: the first with an internal diameter of 50 µm and a length of 20 cm, and the other with an internal diameter of 25 µm and a length of 10 cm. They were respectively 36 and 283 times more resistive than our entire circuit. The unwanted flux generated by pressure disturbances was thus reduced by the same factor. Because our devices were perfused with a syringe pump, these capillary tubes did not affect the repartition of fluid velocity within the chip for a given inflow rate. The loading and fluidisation protocols were also modified, as described in Materials and Methods: the input syringe and outlet tube were connected to the device before cell loading. Inserting either of these two capillary tubes and changing the protocols enabled the cells to stay within the chambers and to be cultured for up to 20 days (**Fig. 4.b**).

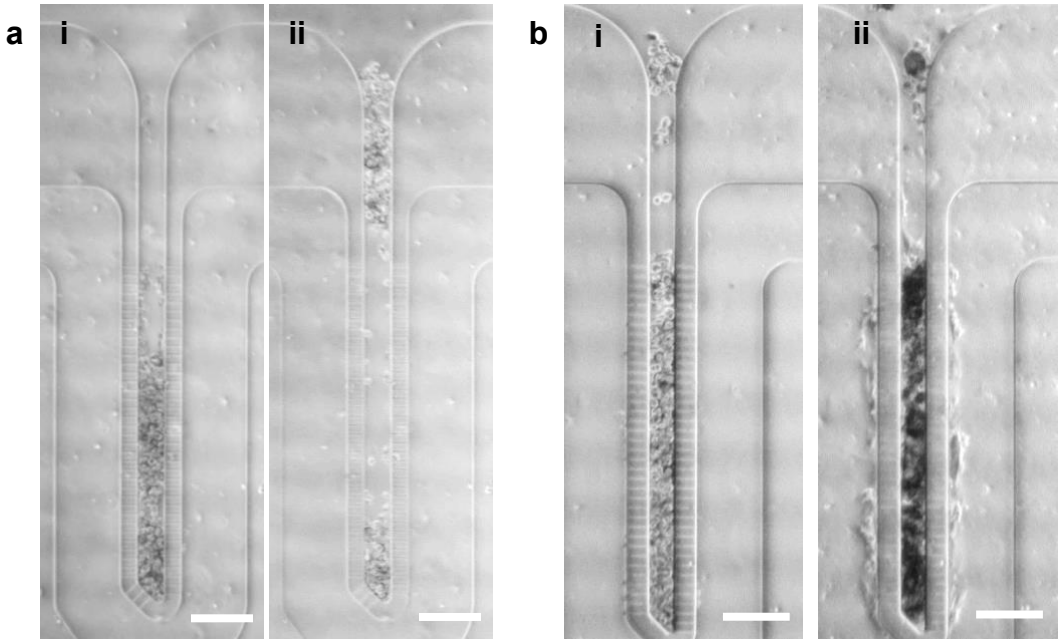

Figure 4. Strategy to adapt cell culture on chip to less adherent HepaRG hepatocytes in the 40-2 µm device. **a**) **i**) After loading onto the device, **ii**) the cells were expelled from the chambers when fluidisation tubes were connected to the chip or when the heights of the syringe and device were modified. **b**) Bright field images **i**) at day 0 and **ii**) at day 20 of cells being loaded and then cultured at 300 nl/min in a device that included external resistances. Scale bars = 100 µm.

Cell distribution and differentiation on the chip

Global cell homogeneity within the chambers of the 40-2 µm device was evaluated by counting cell nuclei from epifluorescence and confocal microscope images at the end of the experiments, after cell fixation and DAPI staining (**Supplementary Fig. S3**). The mean number of cells per chamber was 153±42, so that there was a 30% difference in the cell counts between chambers. The total number of cells on one device reached around 6000.

DAPI staining of the nuclei of HepaRG cells that had been loaded at either the proliferative or differentiated stages was performed and highlighted the satisfactory condition of the cells. Indeed, the nuclei appeared to be regular and round in shape. Almost no apoptotic or necrotic nuclei were noted, indicating that the cells were alive after 14 or 20 days of culture on the chip (**Fig. 5**).

Immunofluorescence assays revealed that after 14 days of culture on the chip, HepaRG cells that had been loaded as hepatoblasts were producing albumin and some of them were positive for HNF4α labelling, particularly in areas of high cell density (**Fig. 5.a.i.ii.iii**). HNF4α is a transcription factor that is expressed early during hepatoblast differentiation into hepatocytes and regulates albumin gene expression. The presence of these two markers indicated that proliferative HepaRG cells were differentiating spontaneously towards hepatocytes on the chip.

After 20 days of culture on the chip, already differentiated HepaRG cells were still producing albumin. In addition, some cells exhibited ZO-1 labelling, indicative of the presence of tight junctions. Its co-localisation with phalloidin staining (targeting F-actin filaments) at some points suggested strong interactions and the polarization of cells (**Fig. 5.a.iv.v**). These cells were maintaining their differentiation and function after a long period of 20 days on the device. In both cases, some binucleated cells were visible, which was also an indication of their

differentiation into hepatocytes. From confocal stacks, we evidenced that cells loaded at both differentiation stages aggregated and took on a 3D organisation within the chambers, with stacks of up to three cells (**Fig. 5.b**).

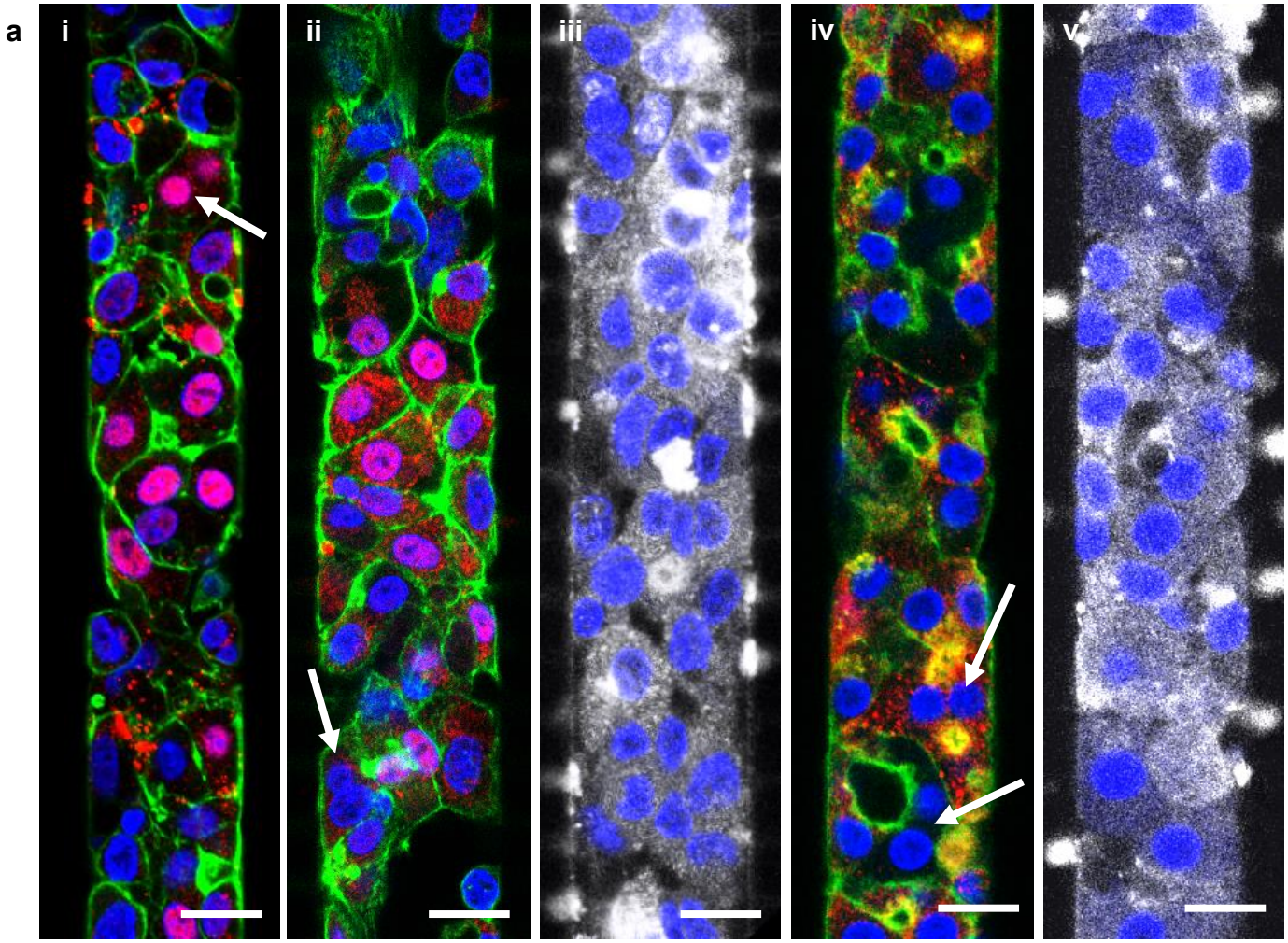
a
i
ii
iii
iv
v

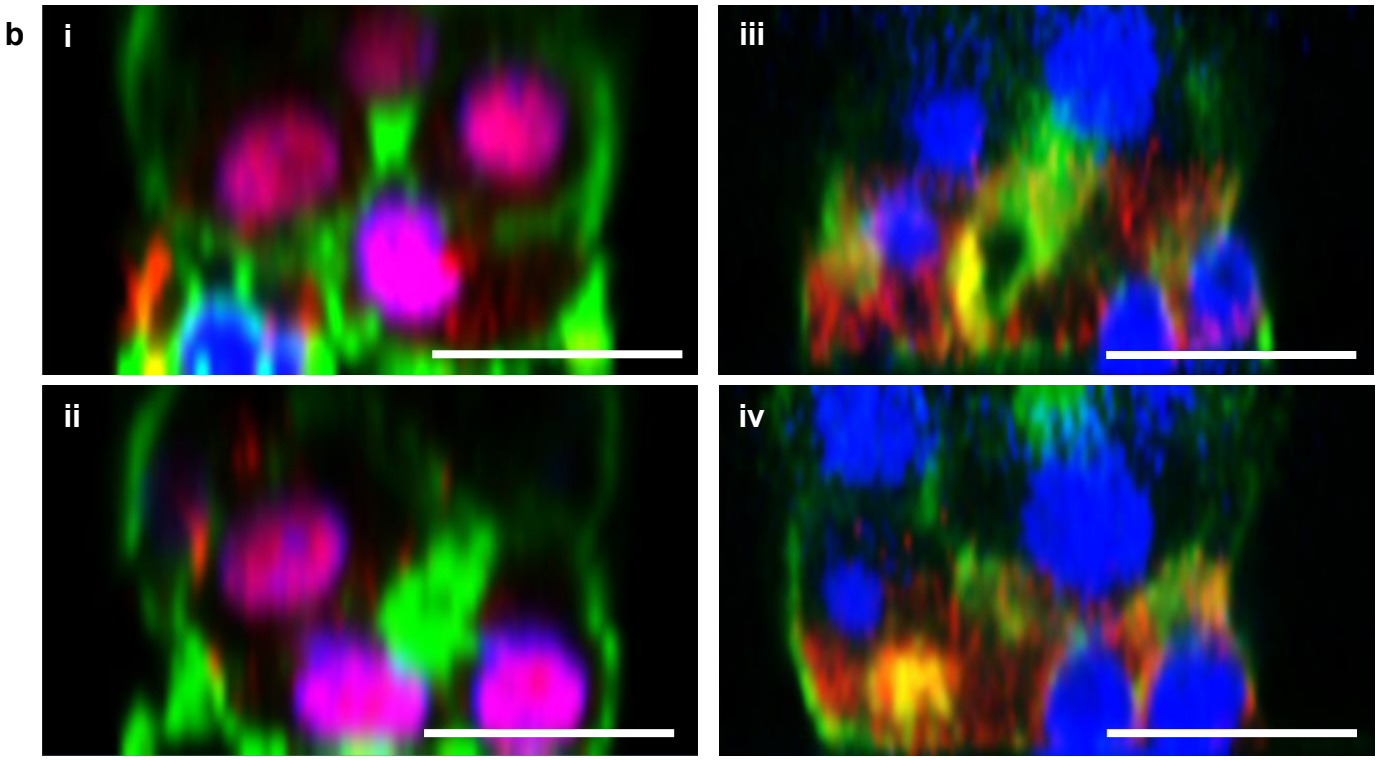
b
i
iii
ii
iv

Figure 5. Immunofluorescence staining of HepaRG cells cultured under different conditions on the 40-2 µm device, revealed under a confocal microscope. **a**) Top-down views of the chamber with respect to: **i**) proliferative HepaRG cells loaded and cultured at 50 nl/min for 14 days, fixed and stained for nuclei (blue), F-actin (green), HNF4α (red); **ii**) and **iii**) proliferative HepaRG cells loaded and cultured at 375 nl/min for 14 days, fixed and stained for nuclei (blue), F-actin (green), HNF4α (red) and albumin (grey); **iv**) and **v**) HepaRG hepatocytes loaded and cultured at 300 nl/min for 20 days, fixed and stained for nuclei (blue), F-actin (green), ZO-1 (red), and albumin (grey). Some binucleated cells can also be seen (white arrows). **b**) Cross-sectional views along the chamber: **i**) and **ii**) correspond to the chamber described in a.i); **iii**) and **iv**) correspond to the chamber described in a.iv). Scale bars = 20 µm.

Discussion

Our microfluidic chip was designed to mimic the microstructure of the liver and enable more physiological culture conditions than other previous devices. Indeed, as well as achieving the 3D culture of hepatocytes, our architecture also allowed the cells to spatially organise into hepatocyte cords with *in vivo* like dimensions. Compared to previous studies describing the same microarchitecture, we were able to culture and analyse a larger number of hepatocyte cord-like structures on a single device[15,16]. For the first time, this architecture was then used to culture human HepaRG cells. We chose this hepatic cell line because they share a larger number of metabolic and functional similarities with human primary hepatocytes than the HepG2 and HuH7 cell lines, for instance. Compared to primary hepatocytes, HepaRG cell line offers an almost unlimited stock of hepatocytes of constant quality. Because these cells are widely used at two different differentiation stages[18–23], our approach providing a single but versatile microfluidic tool for their culture, differentiation and maturation, is of crucial importance in applications targeting drug screening and toxicity. Rather than adjusting the biological and chemical conditions, additional and innovative physical modifications were made to render the device compatible with the seeding and culture of either proliferative or differentiated HepaRG cells. Thus, the geometry, resistivity and flow rate of our device were optimised by taking account of the migratory and adherence properties of these two cell types.

Their migratory behaviour and deformability on the chip indicated that HepaRG cells at the hepatoblast-like stage displayed cancerous-like features. Indeed, the capacity for deformation of cancerous cells is commonly characterized by their ability to pass through very thin microchannels[29]. In all cases, channels with a diameter smaller than 5*2 µm^2 were shown to reduce their migration capacity[30]. These results guided our choice of the slit dimensions in our design (2 µm in the 40-2 µm device). But although the cells were better retained within the chambers using 2 µm height slits and increasing the flow rate, cytoplasmic extensions were still growing towards the medium channel. The use of more complex slit networks, including 90° angles, did not prevent these protrusions. Importantly, the filling of slits by cytoplasmic extensions at various flow rates – ranging from 50 to 400 nl/min – was not found to decrease cell viability after at least two weeks of culture on the chip. Cells within the chamber were supplied with sufficient nutrients and oxygen. Our system was therefore suitable for the long-term culture of HepaRG cells loaded at the proliferative stage.

Unlike proliferative HepaRG cells, already differentiated HepaRG-hepatocytes were highly sensitive to the variations in pressure caused by manipulation of the chip. Small changes to tube connections or the hydrostatic pressure applied to chip inlets frequently caused the expulsion of cells from the chambers. This was most likely due to their preferential adherence to each other rather than to the culture substrate of collagen-coated glass and PDMS. Indeed,

the weaker adherence of HepaRG hepatocytes to the substrate compared to proliferative cells was evidenced in a different structure of microfluidic chip[28]. Rather than promoting cell adhesion by chemically coating the channel surfaces, we modified the geometry of the experimental setup in order to resolve this issue. The addition of external capillary tubes with high hydraulic resistance offered an efficient alternative to desensitise the microfluidic device to pressure disturbances[31,32]. We tested two types of external capillaries which increased the resistance of our circuit 36 or 283-fold, respectively. It was found that even the capillary tube with the lowest resistance was sufficient to desensitise the device to pressure variations. Finally, inserting an external resistance and modifying the loading protocol enabled the maintenance of HepaRG hepatocytes within the chambers.

In order to assess the final cell differentiation status and 3D organisation of HepaRG cells after 14 or 20 days of culture in the device, we halted the experiment by fixing the cells and performing immunofluorescence labelling. Confocal microscopy imaging of our liver tissues on the chip was then performed. Thanks to the geometry of the device, and particularly the 40 µm height of the chambers, we observed that hepatocytes had taken on a 3D organisation and maintained their functionalities for more than 14 days. These observations were made at a greater degree of details than for most existing devices. HepaRG cells loaded as hepatoblasts had spontaneously differentiated into hepatocytes, while already differentiated HepaRG hepatocytes had maintained their differentiation status.

The microfluidic system that we have developed and optimised is suitable for the long term culture and differentiation of human hepatocytes, and well adapted to the different migratory and adhesion properties of these cells when seeded at their different levels of differentiation. In this device, hepatocytes take on a 3D organisation and can be cultured under flux for long periods of time. Using this microfluidic chip with hepatocytes from different sources could serve as a new platform for the performance of drug toxicity assays.

Materials & Methods

Manufacture of the device: The device is made of PDMS using a conventional soft lithography technique[33]. Firstly, the design of the two levels of the microfluidic chip was transferred into chromium masks appropriate for use in UV photolithography. A two-level micro-mould made of thick photoresist (SU-8™, Kayaku Advanced Materials, Westborough, MA, USA) was then made using conventional clean room technologies. Details of the durations of the different steps are given in **Supplementary Table S1**. The first layer of the mould was 2 or 5 µm high (depending on the device), and defined the geometry of the slits connecting the hepatocyte chamber to the medium channel. SU-8 2002 or SU-8 2005 was spin-coated (3000 rpm, 300 rpm/s, 30s) on a silicon wafer to obtain an initial layer of 2 or 5 µm, respectively. The wafer was pre-baked at 65°C then 95°C and 65°C prior to UV exposure (365 nm, lamp power of 18 mJ/cm^2), then post-baked at the same temperatures and finally developed (SU-8 Developer, Kayaku Advanced Materials). SU-8 2025 was then spin-coated as a second layer (3000 rpm, 300 rpm/s, 30s for a 25 µm layer or 2000 rpm, 300 rpm/s, 30s for a 40 µm layer), and pre-baked prior to UV exposure and post-bake developing. Finally, the mould was hard baked in an oven (175°C, 2h). To make the PDMS chips, the mould was first incubated with hexamethyldisilazane vapours for 1h to achieve its passivation. PDMS monomer and reagent (SYLGARD 184 Silicone Elastomer, Dow Chemical, Midland, MI, USA) were mixed at 10:1 (v/v), degassed and poured onto the mould, which was baked for 2h at 75°C. The chip was

then peeled off the mould. The four outlet holes were punched using a 1.5 mm puncher. To remove any remaining pieces of PDMS, the chip was sonicated in ethanol (96%) for 30 s and then dried. It was irreversibly bound to a glass coverslip (0.17 mm thick) with an oxygen plasma treatment (18 W, 300 mTorr, 20 s). Tubes about 1cm in length (teflon perfluoroalcoxy alcane (PFA), 0.50 mm internal diameter (ID), 1/16" outer diameter (OD)) were connected to each outlet, sealed using PDMS and baked for 1h at 75°C. Finally, the entire device was sterilized using oxygen plasma for 3 min.

HepaRG™ cell culture: Cells were supplied by Biopredic International and cultured according to their instructions. They were used between passages 15 and 18. The cells were plated at a density of $2x10^4$ cells/cm^2 and cultured with William's E medium supplemented with L-glutamine (2mM) and HepaRG® Growth Medium Supplement with antibiotics (ADD710, Biopredic International, Saint-Grégoire, France). The medium was changed every two to three days. The cells were allowed to reach confluence before they started spontaneous differentiation. After 14 days of culture, the cells were ready to be detached and loaded onto the chip as "proliferative" or "hepatoblast-like" cells. To further differentiate cells towards hepatocytes on culture wells, the supplement was gradually changed to the HepaRG® Differentiation Medium Supplement with antibiotics (ADD720) containing 1.7% DMSO over a two-to-three-day period.

Selective detachment of hepatocytes derived from HepaRG cells: After culture for a total of 28 days, hepatocytes were selectively detached and loaded onto the chip as "differentiated" or "hepatocyte-like" cells. This previously described technique was intended to preferentially collect hepatocytes from the two cell populations with distinct morphologies that are present during a HepaRG culture[34]. Clusters of small refringent cells correspond to hepatocytes and large and spreading cells correspond to cells committed to a biliary fate. The technique consists in incubating them with trypsin-EDTA (0.05%) for 90 s at 37°C, then gently flushing the plates with trypsin to selectively recover small clusters of hepatocytes.

Loading protocol: The chips were prepared at least one day before cell loading so that any bubbles trapped inside the channels would degas. First, the chips were sterilized a second time with ethanol (70%) for 20 min, rinsed with PBS and then coated with collagen I from rat tail (50 µg/ml, C3867, Sigma-Aldrich, Saint-Louis, MI, USA) for 1h at room temperature (RT). They were then filled with the culture medium and stored in the cell incubator at 37°C overnight. On the day of loading, the two outlets from the medium channel of the chip were connected to a negative pressure controller (MFCS™-EZ, Fluigent, Kremlin-Bicêtre, France) (**Supplementary Fig. S4**). A suspension of either proliferative or differentiated HepaRG cells at a concentration of $1x10^7$ cells/ml was transferred into a syringe. Using the syringe and its needle, drops of the cells were deposited into the two cell channel outlets and suction was started (at -25 mbar for the 25-5 µm device and -20 mbar for the 40-2 µm device). Chamber filling was monitored under a microscope. Once all the chambers had been loaded with cells, the suction was slowly turned off and the controller was disconnected from the chip.

Fluidisation protocol: All elements were autoclaved or sterilized with ethanol (70%). The main tubing used was made up of Teflon PFA (0.05 mm ID, 1/16" OD) and connected to the chip through wider tubes (silicone, 1 mm ID, 3 mm OD). After incubation for 6 hours at 37°C following cell loading, a syringe filled with medium was connected to the medium channel inlet. The three outlets of the device were connected to waste. The syringe was placed on a syringe

pump (Low Pressure Syringe Pump neMESYS 290N, CETONI, Korbußen, Germany) and the flow rate was regulated. The medium in the syringe was changed every 2 to 3 days.

Modified loading and fluidisation protocol: To adapt the protocol to differentiated HepaRG cells, as many fluid connections to the chip as possible were made before cell loading. A syringe filled with cell culture medium and an outlet tube to waste were both connected to one end of the medium channel. An external resistance was also inserted between the syringe and the chip. This resistance was a capillary tube with a diameter of 25 or 50 µm and 10 or 20 cm long (tube references 62510 or 65020 respectively, from Cluzeau Info Labo, Sainte-Foy-La-Grande, France). To load the cells, suction was applied through the previously connected outlet tube (**Supplementary Fig. S4**). After disconnecting the pressure controller from the chip, the ends of the cell channel were connected to waste. The chip and waste container were placed in the incubator and the syringe on the syringe pump. A flow rate of 300 nl/min was applied after 1h of static conditions. The medium in the syringe was changed every 2 to 3 days.

Cell staining and observation: All dilutions were performed in phosphate buffered saline (PBS) 1X. The lengths of all steps are detailed in **Supplementary Table S2**. After the culture period, the cells were fixed on the chip with PFA (4%). They were then permeabilised using a solution containing bovine serum albumin (BSA, 1% w/v), EDTA (5.37×10^{-1} µmol/L), and triton-X-100 (0.1% v/v). They were blocked with BSA (3% w/v) and incubated overnight at 4°C with primary antibodies diluted in BSA (1% w/v) (**Supplementary Table S3**). The cells were then washed with a solution of tween 20 (0.1% v/v), and incubated at room temperature for 2h with secondary antibodies diluted in BSA (1% w/v) (**Supplementary Table S3**). They were washed again with the tween solution and finally with milliQ water. Fluorescent images were recorded using either a Thermofisher EVOS microscope or Leica SP8 confocal microscope and analysed using Fiji software[35,36], as detailed in the Supplementary Information.

Analytical calculations and simulations: A 3D COMSOL Multiphysics® model (COMSOL AB, Stockholm, Sweden) was used to estimate the distributions of velocity and shear stress within the device. Twenty chambers in series and containing no cells were modelled. We chose a creeping flow rate for water at 37°C coupled with the transport of dilute species for oxygen. A flow rate was imposed at one inlet of the medium channel. Pressure was set at 0 Pa for the three other outlets. The oxygen consumption rate was set at $q_{O2} = 5 \times 10^{-17}$ mol/s/cell and Michaelis–Menten kinetics were used to describe the reactions within the chambers[11,37–41]. These simulations are detailed in Supplementary Information. To estimate circuit resistivity, we used the electric–hydraulic analogy $\Delta P = R^*Q$, where ΔP is the pressure difference between the inlet and outlet, Q the flow rate and R the hydraulic resistance of the circuit. We divided the structure into a set of resistances and calculated their resistivities using the following approximation[42] : $R = 12^*\mu^*L^*\alpha/(h^*(1-0.63\alpha))$, $\alpha = h/w \leq 1$, with µ the dynamic viscosity of the fluid, L the length of the channel, w its width and h its height. The resistance network was modelled using TINA software (Texas Instrument, Dallas, TX, USA), with voltage sources at all outlets. By knowing the difference in voltage imposed and evaluating the current generated, the resistance of the circuit was found to be 2.56×10^4 Pa.s.mm^{-3} at 37°C. The resistivity of the capillaries used as external resistances was calculated as: $R = 8^* \mu^*L/(\pi^*r^4)$, with µ the dynamic viscosity of the fluid, L the length of the capillary and r its radius.

References

1. Baudy, A. R. *et al.* Liver microphysiological systems development guidelines for safety risk assessment in the pharmaceutical industry. *Lab on a Chip* (2020) doi:10.1039/c9lc00768g.

2. Morgan, S. J. & Elangbam, C. S. Animal Models of Disease for Future Toxicity Predictions. in *Drug Discovery Toxicology: From Target Assessment to Translational Biomarkers* (2016). doi:10.1002/9781119053248.ch18.

3. Kammerer, S. & Küpper, J.-H. Human hepatocyte systems for in vitro toxicology analysis. *J. Cell. Biotechnol.* (2018) doi:10.3233/jcb-179012.

4. Babai, S., Auclert, L. & Le-Louët, H. Safety data and withdrawal of hepatotoxic drugs. *Therapie* (2018) doi:10.1016/j.therap.2018.02.004.

5. Huh, D., Hamilton, G. A. & Ingber, D. E. From 3D cell culture to organs-on-chips. *Trends in Cell Biology* (2011) doi:10.1016/j.tcb.2011.09.005.

6. Zhou, Y., Shen, J. X. & Lauschke, V. M. Comprehensive evaluation of organotypic and microphysiological liver models for prediction of drug-induced liver injury. *Frontiers in Pharmacology* (2019) doi:10.3389/fphar.2019.01093.

7. Ware, B. R. & Khetani, S. R. Engineered Liver Platforms for Different Phases of Drug Development. *Trends in Biotechnology* (2017) doi:10.1016/j.tibtech.2016.08.001.

8. Probst, C., Schneider, S. & Loskill, P. High-throughput organ-on-a-chip systems: Current status and remaining challenges. *Current Opinion in Biomedical Engineering* (2018) doi:10.1016/j.cobme.2018.02.004.

9. Du, Y. *et al.* Mimicking liver sinusoidal structures and functions using a 3D-configured microfluidic chip. *Lab Chip* (2017) doi:10.1039/C6LC01374K.

10. Kang, Y., Rawat, S., Duchemin, N., Bouchard, M. & Noh, M. Human Liver Sinusoid on a Chip for Hepatitis B Virus Replication Study. *Micromachines* (2017) doi:10.3390/mi8010027.

11. Bavli, D. *et al.* Real-time monitoring of metabolic function in liver-on-chip microdevices tracks the dynamics of mitochondrial dysfunction. *Proc. Natl. Acad. Sci.* (2016) doi:10.1073/pnas.1522556113.

12. Bhise, N. S. *et al.* A liver-on-a-chip platform with bioprinted hepatic spheroids. *Biofabrication* (2016) doi:10.1088/1758-5090/8/1/014101.

13. Yu, F. *et al.* A perfusion incubator liver chip for 3D cell culture with application on chronic hepatotoxicity testing. *Sci. Rep.* (2017) doi:10.1038/s41598-017-13848-5.

14. Jang, M., Kleber, A., Ruckelshausen, T., Betzholz, R. & Manz, A. Differentiation of the human liver progenitor cell line (HepaRG) on a microfluidic-based biochip. *J. Tissue Eng. Regen. Med.* (2019) doi:10.1002/term.2802.

15. Lee, P. J., Hung, P. J. & Lee, L. P. An artificial liver sinusoid with a microfluidic endothelial-like barrier for primary hepatocyte culture. *Biotechnol. Bioeng.* (2007) doi:10.1002/bit.21360.

16. Nakao, Y., Kimura, H., Sakai, Y. & Fujii, T. Bile canaliculi formation by aligning rat primary hepatocytes in a microfluidic device. (2011) doi:10.1063/1.3580753.

17. Tascher, G. *et al.* In-Depth Proteome Analysis Highlights HepaRG Cells as a Versatile Cell System Surrogate for Primary Human Hepatocytes. *Cells* (2019) doi:10.3390/cells8020192.

18. Pasqua, M. *et al.* HepaRG Self-Assembled Spheroids in Alginate Beads Meet the Clinical Needs for Bioartificial Liver. *Tissue Eng. - Part A* (2020) doi:10.1089/ten.tea.2019.0262.

19. Hoekstra, R. *et al.* The HepaRG cell line is suitable for bioartificial liver application. *Int. J. Biochem. Cell Biol.* (2011) doi:10.1016/j.biocel.2011.06.011.

20. Gunness, P. *et al.* 3D organotypic cultures of human heparg cells: A tool for in vitro toxicity studies. *Toxicol. Sci.* (2013) doi:10.1093/toxsci/kft021.

21. Yokoyama, Y. *et al.* Comparison of drug metabolism and its related hepatotoxic effects in heparg, cryopreserved human hepatocytes, and HepG2 cell cultures. *Biol. Pharm. Bull.* (2018) doi:10.1248/bpb.b17-00913.

22. Ott, L. M., Ramachandran, K. & Stehno-Bittel, L. An Automated Multiplexed Hepatotoxicity and CYP Induction Assay Using HepaRG Cells in 2D and 3D. *SLAS Discov.* (2017) doi:10.1177/2472555217701058.

23. Guillouzo, A. *et al.* The human hepatoma HepaRG cells: A highly differentiated model for studies of liver metabolism and toxicity of xenobiotics. *Chem. Biol. Interact.* (2007) doi:10.1016/j.cbi.2006.12.003.

24. McCarty, W. J., Usta, O. B. & Yarmush, M. L. A Microfabricated Platform for Generating Physiologically-Relevant Hepatocyte Zonation. *Sci. Rep.* (2016) doi:10.1038/srep26868.

25. Waseem, N. & Chen, P. H. Hypoxic hepatitis: A review and clinical update. *Journal of Clinical and Translational Hepatology* (2016) doi:10.14218/JCTH.2016.00022.

26. Aleksandrova, A. V. *et al.* Mathematical and Experimental Model of Oxygen Diffusion for HepaRG Cell Spheroids. *Bull. Exp. Biol. Med.* (2016) doi:10.1007/s10517-016-3326-1.

27. Khakpour, S. *et al.* Oxygen transport in hollow fibre membrane bioreactors for hepatic 3D cell culture: A parametric study. *J. Memb. Sci.* (2017) doi:10.1016/j.memsci.2017.09.024.

28. Ong, L. J. Y. *et al.* A pump-free microfluidic 3D perfusion platform for the efficient differentiation of human hepatocyte-like cells. *Biotechnol. Bioeng.* (2017) doi:10.1002/bit.26341.

29. Ma, Y.-H. V., Middleton, K., You, L. & Sun, Y. A review of microfluidic approaches for investigating cancer extravasation during metastasis. *Microsystems Nanoeng.* (2018) doi:10.1038/micronano.2017.104.

30. Malboubi, M., Jayo, A., Parsons, M. & Charras, G. An open access microfluidic device for the study of the physical limits of cancer cell deformation during migration in confined environments. *Microelectron. Eng.* (2015) doi:10.1016/j.mee.2015.02.022.

31. Kou, S. *et al.* A multishear microfluidic device for quantitative analysis of calcium dynamics in osteoblasts. *Biochem. Biophys. Res. Commun.* (2011) doi:10.1016/j.bbrc.2011.04.044.

32. Dinh, N. D. *et al.* Preparation of neuronal co-cultures with single cell precision. *J. Vis. Exp.* (2014) doi:10.3791/51389.

33. McDonald, J. C. & Whitesides, G. M. Poly(dimethylsiloxane) as a material for fabricating microfluidic devices. *Acc. Chem. Res.* (2002) doi:10.1021/ar010110q.

34. Laurent, V. *et al.* Highly efficient SiRNA and gene transfer into hepatocyte-like HepaRG cells and primary human hepatocytes: New means for drug metabolism and toxicity studies. *Methods Mol. Biol.* (2013) doi:10.1007/978-1-62703-321-3_25.

35. Schindelin, J. *et al.* Fiji: An open-source platform for biological-image analysis. *Nature Methods* (2012) doi:10.1038/nmeth.2019.

36. Čapek, M., Janáček, J. & Kubínová, L. Methods for compensation of the light attenuation with depth of images captured by a confocal microscope. *Microsc. Res. Tech.* (2006) doi:10.1002/jemt.20330.

37. Nahmias, Y. *et al.* A novel formulation of oxygen-carrying matrix enhances liver-specific function of cultured hepatocytes. *FASEB J.* (2006) doi:10.1096/fj.06-6192fje.

38. Matsumoto, S. *et al.* Integration of an oxygen sensor into a polydymethylsiloxane hepatic culture device for two-dimensional gradient characterization. *Sensors Actuators, B Chem.* (2018) doi:10.1016/j.snb.2018.05.053.

39. Grünig, D., Felser, A., Bouitbir, J. & Krähenbühl, S. The catechol-O-methyltransferase inhibitors tolcapone and entacapone uncouple and inhibit the mitochondrial respiratory chain in HepaRG cells. *Toxicol. Vitr.* (2017) doi:10.1016/j.tiv.2017.05.013.

40. Peyta, L. *et al.* Reduced cardiolipin content decreases respiratory chain capacities and increases ATP synthesis yield in the human HepaRG cells. *Biochim. Biophys. Acta - Bioenerg.* (2016) doi:10.1016/j.bbabio.2016.01.002.

41. Evenou, F., Fujii, T. & Sakai, Y. Spontaneous Formation of Highly Functional Three-Dimensional Multilayer from Human Hepatoma Hep G2 Cells Cultured on an Oxygen-Permeable Polydimethylsiloxane Membrane.

42. Tanyeri, M., Ranka, M., Sittipolkul, N. & Schroeder, C. M. A microfluidic-based hydrodynamic trap: Design and implementation Flow in a rectangular channel. *Lab Chip* **11**, 1786–1794 (2011).

Legends

Figure 1. Design of the microfluidic device. **a**) Zoom on three chambers. The cell channel and hepatocyte chambers (yellow) communicate with the medium channel (pink) via an array of slits (orange). The direction of medium flow is represented by pink arrows. Scale bar = 100 µm. **b**) Top-down view of the design which comprises two fluidic circuits: in pink the medium channel and in yellow the cell channel. Scale bar = 3 mm. **c**) Fluidisation of the chip: the flow enters from one inlet of the

medium channel (red arrow) and leaves via three outlets. Scale bar = 3 mm. **d**) Side-on diagram of the device: a polydimethylsiloxane (PDMS) chip (orange) is sealed to a glass slide (grey), thus creating microfluidic channels (pink). Depending on the different versions of the device, the slits are 2 or 5 µm high and the other channels are 25 or 40 µm high.

Figure 2. Evidence for the migration of proliferative HepaRG cells out of culture chambers determined by phase contrast imaging and fluorescent staining (blue: DAPI, green: phalloidin, staining cell nuclei and F-actin filaments, respectively). **a**) Epifluorescence microscope images of a chamber on the 25-5 µm device after 2 days under static conditions. The migration of cell nuclei through slits was observed (white arrows). **b**) Epifluorescence microscope images of a chamber on the 40-2 µm device after 14 days at 50 nl/min. **c**) Confocal microscope images of a chamber on the 40-2 µm device after 14 days at 50 nl/min: **i**) with straight slits or **ii**) with discontinuous slits. Scale bars = 40 µm.

Figure 3. Numerical modelling of the culture conditions for cells on the 40-2 µm chip. 3D COMSOL® simulation of 20 chambers in a series with straight slits, without any cells, at 37°C. The flow rate at the inlet (symbolized by black arrows) is 400 nl/min. At the three outlets the pressure is set at 0 Pa. **a**) Fluid velocity on the xy plan (z = 20 µm) for chambers 1, 10, and 20. Scale bar = 100 µm. **b**) Shear stress on the xy plan (z = 0 µm). Left-hand side: general view of the first chamber, scale bar = 100 µm. Right-hand side: zoom on the dead-end portion of chambers 1, 10, and 20. Scale bar = 40 µm. **c**) Table of the mean values for velocity and shear stress inside chambers 1, 10, and 20.

Figure 4. Strategy to adapt cell culture on chip to less adherent HepaRG hepatocytes in the 40-2 µm device. **a**) **i**) After loading onto the device, **ii**) the cells were expelled from the chambers when fluidisation tubes were connected to the chip or when the heights of the syringe and device were modified. **b**) Bright field images **i**) at day 0 and **ii**) at day 20 of cells being loaded and then cultured at 300 nl/min in a device that included external resistances. Scale bars = 100 µm.

Figure 5. Immunofluorescence staining of HepaRG cells cultured under different conditions on the 40-2 µm device, revealed under a confocal microscope. **a**) top-down views of the chamber with respect to: **i**) proliferative HepaRG cells loaded and cultured at 50 nl/min for 14 days, fixed and stained for nuclei (blue), F-actin (green), HNF4α (red); **ii**) and **iii**) proliferative HepaRG cells loaded and cultured at 375 nl/min for 14 days, fixed and stained for nuclei (blue), F-actin (green), HNF4α (red) and albumin (grey); **iv**) and **v**) HepaRG hepatocytes loaded and cultured at 300 nl/min for 20 days, fixed and stained for nuclei (blue), F-actin (green), ZO-1 (red), and albumin (grey). Some binucleated cells can also be seen (white arrows). **b**) Cross-sectional views along the chamber: **i**) and **ii**) correspond to the chamber described in a.i); **iii**) and **iv**) correspond to the chamber described in a.iv). Scale bars = 20 µm.

Acknowledgments

This work as well as MB's PhD fellowship and AM's postdoctoral position were funded by RHU program "iLite" on "innovations for Liver tissue engineering" granted by PAI2 through ANR-16-RHUS-0005.

Author contributions

M.B.: designed and conducted experiments, reviewed and interpreted the results and drafted and finalised the manuscript. N.B.: provided experimental advice and participation, reviewed and interpreted the results and finalised the manuscript. A.M.: provided experimental advice, reviewed and interpreted the results and finalised the manuscript. R.G.: conducted chip mould protocol optimisation. I.BM.:

supplied cells and culture media. JC.DV: developed the study concept and study design, interpreted the results and finalised the manuscript. A.D-K.: developed the study concept and study design, interpreted the results and drafted and finalised the manuscript. B.L-P: developed the study concept and study design, interpreted the results, and drafted and finalised the manuscript.

Additional information

The author(s) declare no competing interests.

Data availability

The datasets generated during and/or analysed during the current study are available from the corresponding author on reasonable request.

Figures

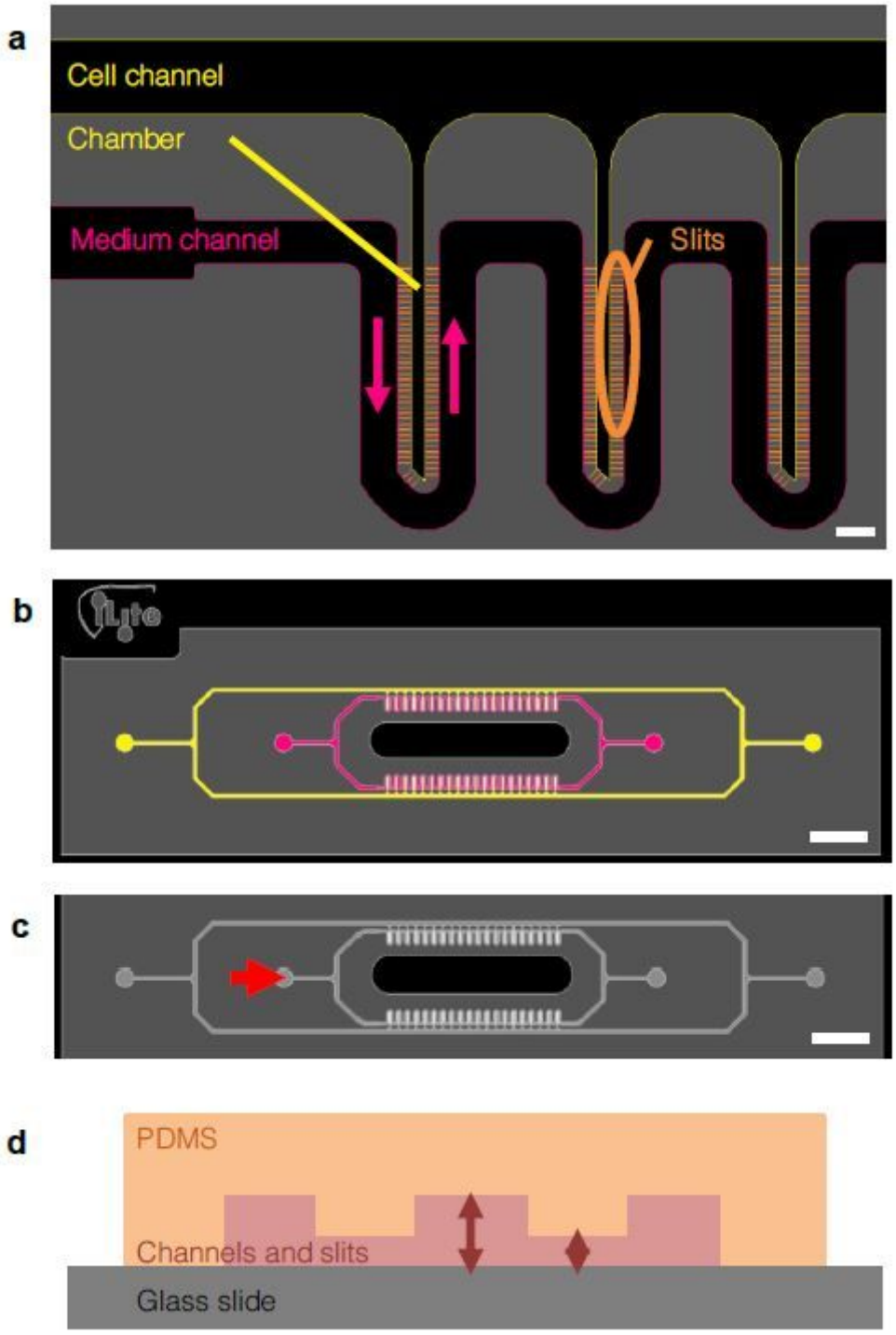

Figure 1

Design of the microfluidic device. a) Zoom on three chambers. The cell channel and hepatocyte chambers (yellow) communicate with the medium channel (pink) via an array of slits (orange). The direction of medium flow is represented by pink arrows. Scale bar = 100 µm. b) Top-down view of the

design which comprises two fluidic circuits: in pink the medium channel and in yellow the cell channel. Scale bar = 3 mm. c) Fluidisation of the chip: the flow enters from one inlet of the medium channel (red arrow) and leaves via three outlets. Scale bar = 3 mm. d) Side-on diagram of the device: a polydimethylsiloxane (PDMS) chip (orange) is sealed to a glass slide (grey), thus creating microfluidic channels (pink). Depending on the different versions of the device, the slits are 2 or 5 µm high and the other channels are 25 or 40 µm high.

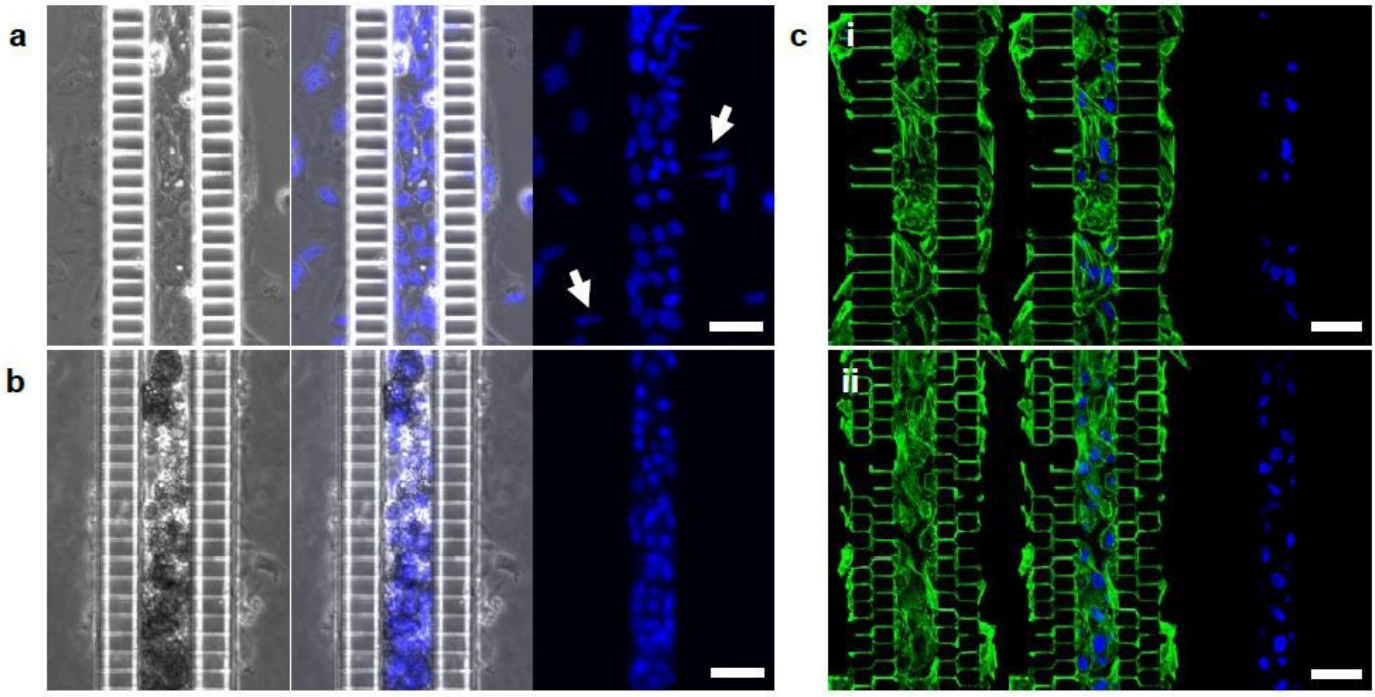

Figure 2

Evidence for the migration of proliferative HepaRG cells out of culture chambers determined by phase contrast imaging and fluorescent staining (blue: DAPI, green: phalloidin, staining cell nuclei and F-actin filaments, respectively). a) Epifluorescence microscope images of a chamber on the 25-5 µm device after 2 days under static conditions. The migration of cell nuclei through slits was observed (white arrows). b) Epifluorescence microscope images of a chamber on the 40-2 µm device after 14 days at 50 nl/min. c) Confocal microscope images of a chamber on the 40-2 µm device after 14 days at 50 nl/min: i) with straight slits or ii) with discontinuous slits. Scale bars = 40 µm.

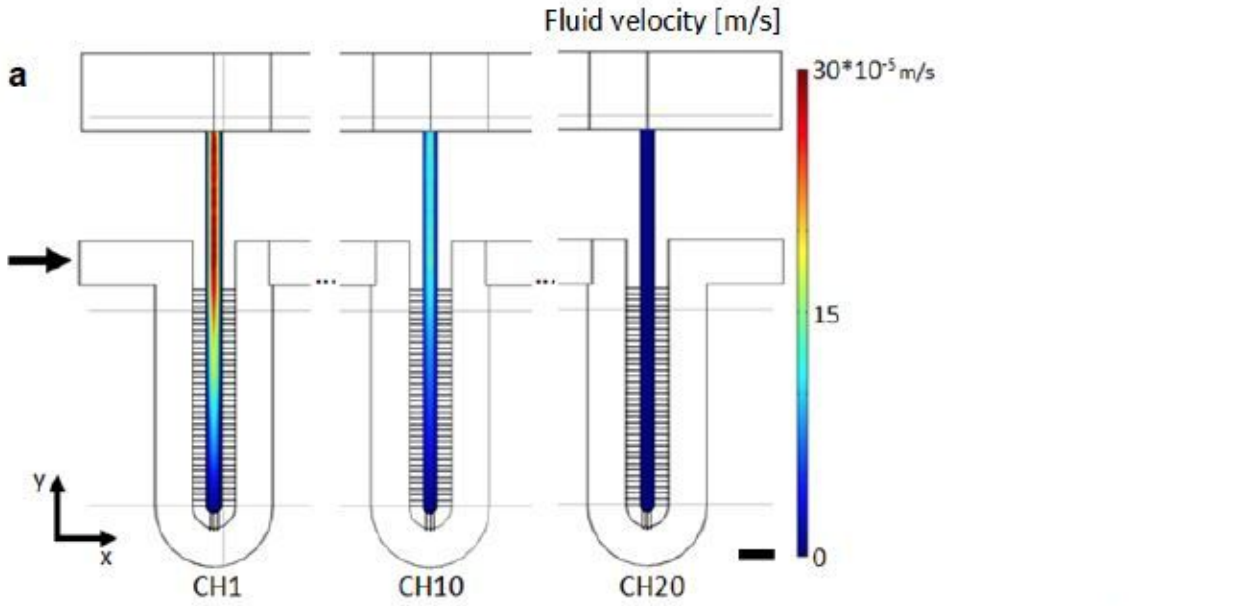

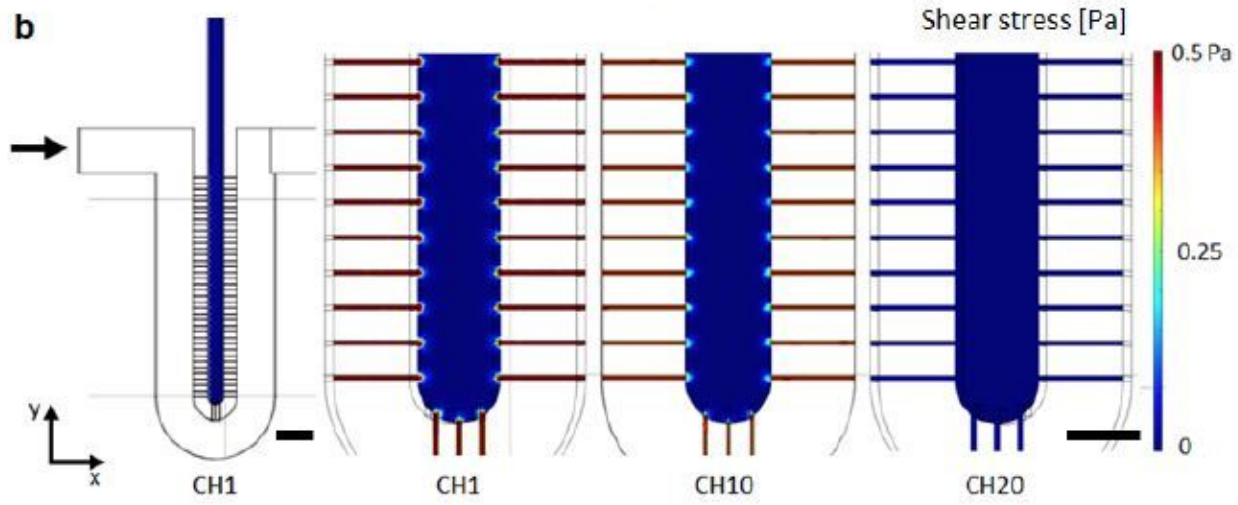

c

400 nl/min	Mean velocity [m/s]	Mean shear stress [Pa]
40-2 device		
Chamber n°1	9.08e-5	2.1e-2
Chamber n°10	3.98e-5	9.0e-3
Chamber n°20	1.97e-5	4.0e-4

Figure 3

Numerical modelling of the culture conditions for cells on the 40-2 µm chip. 3D COMSOL® simulation of 20 chambers in a series with straight slits, without any cells, at 37°C. The flow rate at the inlet (symbolized by black arrows) is 400 nl/min. At the three outlets the pressure is set at 0 Pa. a) Fluid velocity on the xy plan (z = 20 µm) for chambers 1, 10, and 20. Scale bar = 100 µm. b) Shear stress on the xy plan (z = 0 µm). Left-hand side: general view of the first chamber, scale bar = 100 µm. Right-hand side:

zoom on the dead-end portion of chambers 1, 10, and 20. Scale bar = 40 µm. c) Table of the mean values for velocity and shear stress inside chambers 1, 10, and 20.

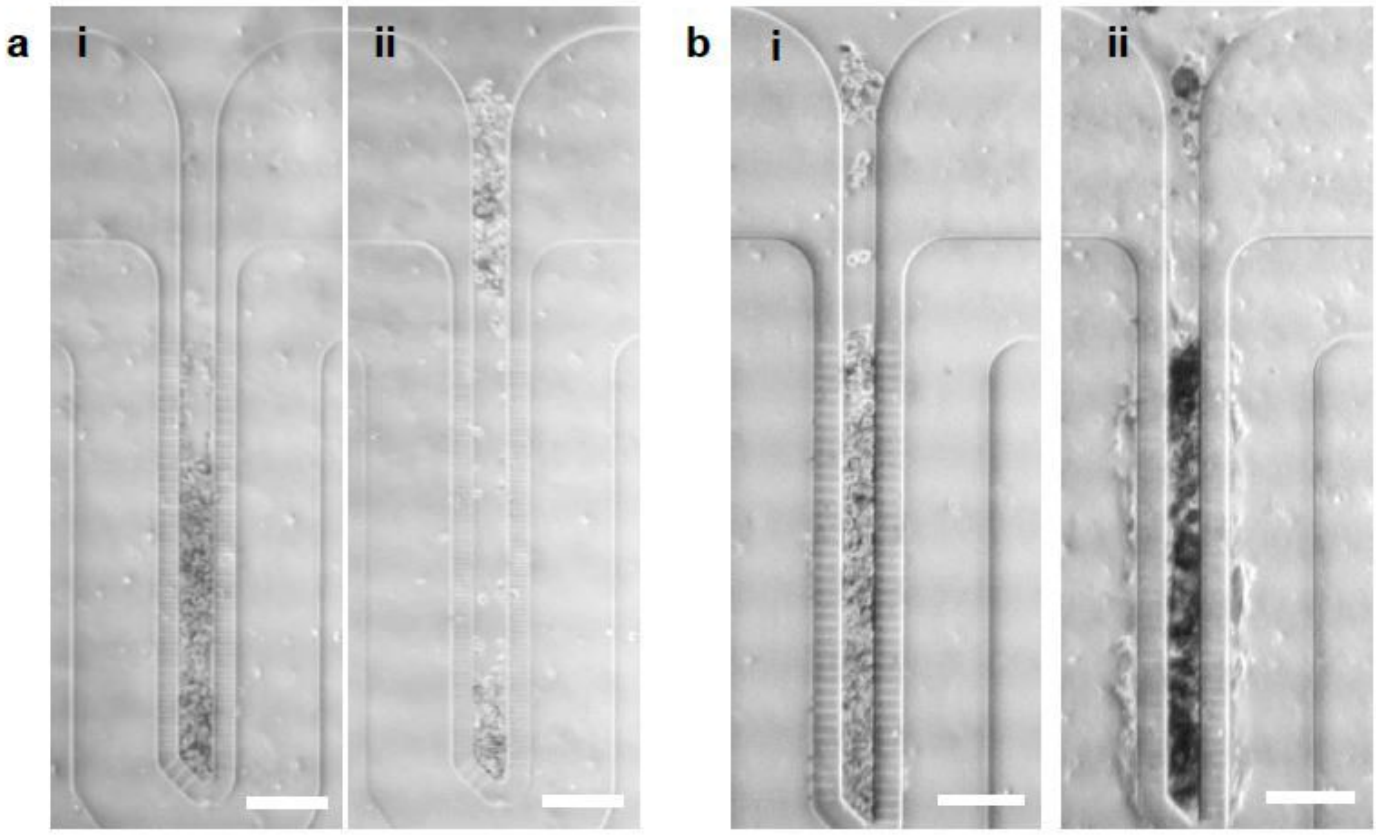

Figure 4

Strategy to adapt cell culture on chip to less adherent HepaRG hepatocytes in the 40-2 µm device. a) i) After loading onto the device, ii) the cells were expelled from the chambers when fluidisation tubes were connected to the chip or when the heights of the syringe and device were modified. b) Bright field images i) at day 0 and ii) at day 20 of cells being loaded and then cultured at 300 nl/min in a device that included external resistances. Scale bars = 100 µm.

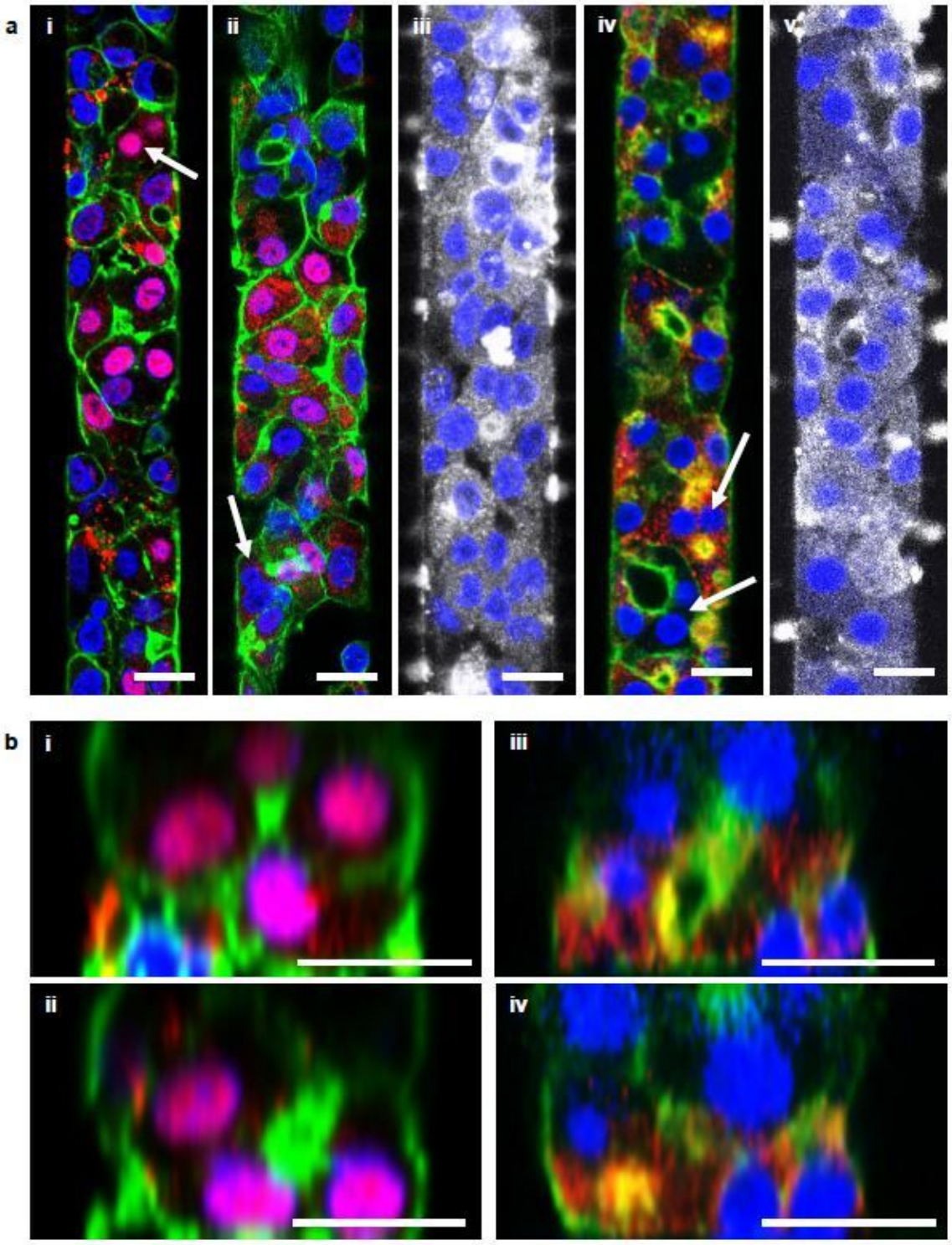

Figure 5

Immunofluorescence staining of HepaRG cells cultured under different conditions on the 40-2 μm device, revealed under a confocal microscope. a) top-down views of the chamber with respect to: i) proliferative HepaRG cells loaded and cultured at 50 nl/min for 14 days, fixed and stained for nuclei (blue), F-actin (green), HNF4α (red); ii) and iii) proliferative HepaRG cells loaded and cultured at 375 nl/min for 14 days, fixed and stained for nuclei (blue), F-actin (green), HNF4α (red) and albumin (grey); iv) and v) HepaRG

hepatocytes loaded and cultured at 300 nl/min for 20 days, fixed and stained for nuclei (blue), F-actin (green), ZO-1 (red), and albumin (grey). Some binucleated cells can also be seen (white arrows). b) Cross-sectional views along the chamber: i) and ii) correspond to the chamber described in a.i); iii) and iv) correspond to the chamber described in a.iv). Scale bars = 20 μm.

Supplementary Files

This is a list of supplementary files associated with this preprint. Click to download.

- BoulScienticRepSupplementary.pdf